Electrochemical and Monte Carlo studies of self-assembled trans-[Fe(cyclam)(NCS)2]+ complex ion on gold surface as electrochemical sensor for nitric oxide

ARTICLE *in* ELECTROCHIMICA ACTA · FEBRUARY 2013

Impact Factor: 4.5 · DOI: 10.1016/j.electacta.2012.11.132

Electrochimica Acta 91 (2013) 1–10

Contents lists available at SciVerse ScienceDirect

Electrochimica Acta

journal homepage: www.elsevier.com/locate/electacta

Electrochemical and Monte Carlo studies of self-assembled *trans*-[Fe(cyclam)(NCS)$_2$]$^+$ complex ion on gold surface as electrochemical sensor for nitric oxide

Vanessa N. Santos[a], Glaydson L.F. Mendonça[a], Valder N. Freire[c], Alda K.M. Holanda[b], Jackson R. Sousa[b], Luiz G.F. Lopes[b], Javier Ellena[d], Adriana N. Correia[a], Pedro de Lima-Neto[a,*]

[a] Departamento de Química Analítica e Físico-Química, Universidade Federal do Ceará, Campus do Pici, Bloco 940, 60455-960, Fortaleza, CE, Brazil
[b] Departamento de Química Orgânica e Inorgânica, Universidade Federal do Ceará, Cx. Postal 12200, Cep 60455-960 Fortaleza, CE, Brazil
[c] Departamento de Física, Universidade Federal do Ceará, Campus do Pici, C.P. 6030, 60455-960 Fortaleza, CE, Brazil
[d] Instituto de Física de São Carlos, Universidade de São Paulo, C.P. 369, 13560-970 São Carlos, SP, Brazil

ARTICLE INFO

Article history:
Received 7 August 2012
Received in revised form
24 November 2012
Accepted 29 November 2012
Available online 21 December 2012

Keywords:
Monte Carlo
Electrochemical sensor
Characterization
Fe–cyclam complex
NO detection

ABSTRACT

Modification of gold electrode by self-assembled *trans*-[Fe(cyclam)(NCS)$_2$]$^+$ complex ion to produce an electrochemical sensor for nitric oxide detection was investigated. Dopamine, serotonin and nitrite were examined as interferents. The synthesized complex was characterized by X-ray diffraction and by infrared spectroscopy. The modified electrode was characterized by cyclic voltammetry and by surface enhanced Raman spectroscopy, analytical curves were obtained by square wave voltammetry and Monte Carlo calculations were made to model the interaction of NO molecules with the unmodified and modified surfaces. The complex has distorted octahedron geometry with the thiocyanate groups bonded to the iron ion by the nitrogen atom and in the *trans* orientation. SERS spectrum and Monte Carlo calculations supported that the complex ion is adsorbed on Au surface from the Au-S bond. The electrochemical current for NO oxidation on the modified electrode was higher than that presented by the bare Au electrode and a good correlation was presented by the experimental analytical curve and the calculated Monte Carlo interaction energy versus amount NO molecules plot. The Monte Carlo calculations indicated that the higher current response for NO oxidation on the Au/*trans*-[Fe(cyclam)(NCS)$_2$]$^+$ surface was due to the stronger interaction of the NO molecules with complex adsorbed on the Au surface than the interaction of NO with the bare Au surface. The theoretical analyses also revealed that NO molecules cluster on Au surface. Dopamine, serotonin and nitrite were interferents for the detection of NO with dopamine and serotonin was less significant interferents than the nitrite. The proposed modified electrode presented good electrochemical stability, detection limit and quantification limit of 5.15×10^{-8} mol L^{-1} and 1.72×10^{-7}, respectively, which were about one order of magnitude lesser than the corresponding values obtained for the bare Au electrode. The results indicated that the proposed electrode has potential to be applied as a sensor for NO detection.

1. Introduction

Nitric oxide (NO) is a small gaseous molecule that has a remarkable aspect of the ability to be beneficial or toxic according to its concentration in biological medium, since it is associated with many physiological and pathological processes [1–3]. It is known as a vasodilator endothelial regulator of blood pressure, anticoagulants and activator of the vascular system, as well as mediator of antimicrobial and antitumor activities. It can also be identified as a neurotransmitter in the nervous system and a cytotoxic factor in the immune system [4,5]. Since their beneficial and deleterious effects are related with its concentration in biological medium, the development of new methods for the measurement of NO at biologically relevant concentrations has also been a research area of considerable interest.

The NO molecule is known as an unstable molecule, since it presents a short half-life of 0.1 to 6 s, it has high chemical activity, it is presented in biological medium in concentration range covering from 10^{-12} mol L^{-1} to 10^{-6} mol L^{-1} [3], it reacts with other biological components such as hemoglobin or oxygen generating nitrite (NO^{2-}) and nitrate (NO^{3-}) [4,5]. All these aspects make the development of analytical procedures for NO detection a challenge.

Electrochemical techniques provide the possibility to overcome this challenge because they allow detecting NO in real-time, on-line

* Corresponding author. Tel.: +55 85 33669956; fax: +55 85 33669982.
E-mail address: plimaneto@yahoo.com.br (P. de Lima-Neto).

0013-4686/$ – see front matter © 2012 Elsevier Ltd. All rights reserved.
http://dx.doi.org/10.1016/j.electacta.2012.11.132

and in vivo. In addition, they have presented significant advantages over others methodologies because they are quick, simple and present good sensitivity and good selectivity [6]. One of the most widely used strategies is to design electrochemical sensors from the modification of an electrodic surface, such as gold or glassy carbon, with a molecular material, such as metal complexes. An overview of designing molecular material and strategies for the electrochemical detection of nitric oxide in biological media, in addition to other molecules, such as superoxide and peroxynitrite is reported in the literature by Bedioui et al. [7].

Three important considerations should be taken into account when selecting a molecular material to building up an electrochemical sensor for in vivo determination of NO: it should be able to determine NO in presence of interfering ion, such as NO^{2-}, and neurotransmitters, it should be biocompatible and it should be chemically stable in biological medium. Due to these motifs, it is currently crescent the interest to study metal macrocyclic complexes as modifier of the electrode surface in order to obtain an electrochemical sensor for NO and metallophthalocyanine and metalloporphyrin are the most commonly used for this intention [8–15].

Our group has reported that Ru-based [16–21] and Fe-based [22–26] complexes can act as donors or as scavengers of nitric oxide because they are know to present reversible binding with NO. In addition, Mori et al. [27] have shown that gold electrodes modified with molybdenum oxide and *trans*-$[Ru(NH_3)_4(SO_4)_4pic]^+$ can be applied to monitor real-time changes in NO concentrations at low levels. Recently, we reported that the modification of the gold electrode by the *trans*-$Ru[(NH_3)_4(Ist)SO_4]^+$ ion complex, where (Ist) is the thioisonicotinamide ligand, has potential to be applied as a sensor for NO [28]. Thus, these two last reports indicate that the metal complexes that present reversible binding with NO have potential to be molecular materials to modify electrode surfaces to design new electrochemical sensors for detection of NO. Therefore, our interest to study Fe–cyclam based complex as molecular material with the intention to obtain an electrochemical sensor for NO is related to the fact these compounds presents reversible binding with NO [24,26]. In addition, for the best of our knowledge, no attention is given for tetrazamacrocyclic ligands such as cyclam (1,4,8,11-tetraaza-ciclotetradecano) and their metal complexes as modifier of the electrode surface to detect NO.

In recent years, computational modeling has emerged as a powerful tool to study the interaction of molecules with surfaces, thanks to the technological evolution of software and the hardware. The improvement of the computational techniques reflects the quality of the calculation and the possibility of extending the calculations to systems of chemical interest, especially those of medium size systems, particularly when methodologies are employed at high level (ab initio and functional density). Theoretical chemical methods have shown to be useful in determining the molecular structure as well as elucidation of the atomic structure and reactivity of different molecules. However, until now it is not given attention to the use of computational methods, classical or ab initio, to model electrochemical sensors, since the evaluation of the efficiency of a sensor using computational methods may allow the development of models in which several calculated chemical properties can be related to the real power of detection without the need for experimental costs. Among the existent computational methods, Monte Carlo method is useful for the determination of physical properties of chemical interest and it makes use of statistical models and resolution of all randomized trial well behaved wave functions (continuous, normalized and with continuous partial derivatives). The fundamentals of this method are associated with the works of Metropolis et al. [29] and Alder and Wainwright [30].

Thus, the aim of this study is to investigate the self-assembled *trans*-$[Fe(cyclam)(NCS)_2]^+$ layer on gold surface in order to evaluate this modified electrode as a sensor for NO detection using electrochemical techniques and Monte Carlo computational simulation. Thiocyanate was selected because it is known that the chemical bond of the sulfur atom with the gold atom allows a good stability of the adsorbed layer.

2. Experimental

2.1. Chemicals and reagents

Cyclam (1,4,8,11-tetraazacyclotetradecane) was obtained from Aldrich and used without further purification. Na_2SO_4 (J.T. Baker) and sulfuric acid (Suprapur–Merck) were used as received. The *cis*-[(cyclam)$FeCl_2$]Cl complex was prepared according to the literature procedure [24,31]. All other chemicals were of analytical grade and Millipore-Q purified water was used to prepare all solutions, which, previously to the experiments, were deaerated with high-purity N_2 (White Martins SS) and the experiments were carried out at room temperature.

2.2. Preparation of trans-[Fe(cyclam)(NCS)$_2$](PF$_6$)

The complex *trans*-$[Fe(cyclam)(NCS)_2](PF_6)$ was prepared by dissolving 0.100 g (0.263 mmol) of *trans*-[Fe(cyclam)$FeCl_2$]Cl and 0.026 g of solid KCNS in 10 mL of water. The mixture was then allowed to react for 30 min, with stirring. The reaction solution was then concentrated by rotary evaporation under vacuum until the volume reach near to 2 cm^3. Precipitation was induced by the addition of 2 cm^3 of an aqueous saturated solution of NH_4PF_6. Red crystals of the *trans*-$[Fe(cyclam)(NCS)_2](PF_6)$ complex were grown by the standard slow evaporation method of recrystallization and they were suitable for X-ray analysis.

2.3. Modification of the Au electrode surfaces

Initially, the gold electrode was mechanically polished with alumina (0.1 μm), rinsed with Milli-Q water and sonicated in an ultrasonic bath for 10 min. In order to remove possible contamination, the polycrystalline gold electrode was immersed in H_2SO_4 and H_2O_2 (3:1 (v/v)) for 3 min and rinsed thoroughly with water, followed by cyclic potential sweep at 0.1 V s^{-1} from 0.0 V to 1.65 V (E vs. Ag/AgCl, saturated KCl) range in a 1.0 mol L^{-1} H_2SO_4. After this procedure, the polycrystalline Au electrode was immersed in 0.2 mol L^{-1} Na_2SO_4 solution containing 0.01 mol L^{-1} *trans*-$[Fe(cyclam)(NCS)_2]^+$ complex ion for different immersion times in order to carry out the film formation of the complex ion on the gold electrode surface (Au/*trans*-$[Fe(cyclam)(NCS)_2]^+$). The successful of the electrode modification was assessed by cyclic voltammetry of the modified electrode in the supporting electrolyte. In order to optimize the modification time for NO detection, cyclic voltammograms for the gold electrode modified at different immersion time were obtained in 0.2 mol L^{-1} Na_2SO_4 solution containing 1.14×10^{-5} mol L^{-1} NO.

2.4. Apparatus

Infrared spectra were obtained in KBr pellets with a Shimadzu IR Prestige-21 spectrophotometer. All the voltammetric measurements were taken with a potentiostat (Autolab PGSTAT 30, Metrohm-Eco Chemie) linked to a personal computer, using GPES version 4.9 software (General Purpose Electrochemical System, Metrohm-Eco Chemie). A conventional cell with a three-electrode system, consisting of an Ag/AgCl/Cl^- saturated electrode as the reference electrode, a Pt wire as the auxiliary electrode, and a gold polycrystalline electrode of 0.07 cm^2, with and without

Table 1
Crystal data and details of the structure determination for *trans*-[Fe(cyclam)(NCS)$_2$](PF$_6$).

Empirical formula	$C_{12}H_{24}N_6F_6PS_2Fe$	
Formula weight	517.31	
Temperature	293(2) K	
Wavelength	0.71073 Å	
Crystal system	Triclinic	
Space group	P-1	
Unit cell dimensions	a = 7.7290(6) Å	α = 65.814(4)°
	b = 8.5770(9) Å	β = 70.481(6)°
	c = 9.0590(9) Å	γ = 82.078(6)°
Volume	516.34(8) Å3	
Z	1	
Density (calculated)	1.664 Mg/m^3	
Absorption coefficient	1.074 mm^{-1}	
F(000)	265	
Crystal size	0.14 × 0.04 × 0.02 mm^3	
Theta range for data collection	3.17–25.46°	
Index ranges	$-9 \le h \le 9$, $-7 \le k < \le 10$, $-8 \le l \le 10$	
Reflections collected	2840	
Independent reflections	1862 [R(int) = 0.0455]	
Completeness to theta = 25.46°	97.3%	
Absorption correction	Semi-empirical from equivalents	
Max. and min. transmission	0.854 and 0.805	
Refinement method	Full-matrix least-squares on F^2	
Computing [a]	COLLECT[2], HKL Denzo and Scalepack[3]	
SHELXS-97[4], SHELXL-97[5]		
Data/restraints/parameters	1862/0/160	
Goodness-of-fit on F^2	1.042	
Final R indices [$I > 2\sigma(I)$]	R1 = 0.0494, wR2 = 0.0927	
R indices (all data)	R1 = 0.0950, wR2 = 0.1080	
Largest diff. peak and hole	0.396 and −0.432 e Å^{-3}	

[a] Data collection, data processing, structure solution and structure refinement respectively.

modification, and laterally covered with inert material (Teflon) as working electrode.

Single crystals of the complex were used for data collection and cell parameter determination on an Enraf-Nonius Kappa-CCD diffractometer, using Mo Kα radiation (k = 0.71073 Å). Data collection was made by using the COLLECT program [32]; integration and scaling of the reflections were performed with the HKL Denzo-Scalepack system of programs [33]. Absorption corrections were carried out by using the multi-scan method [34].The structure was solved by direct methods with SHELXS-97 [35]. The models were refined by full-matrix least-squares on F^2 with SHELXL-97 [36]. All the hydrogen atoms were stereochemically positioned and refined with the riding model [37]. A summary of the fundamental structural parameters of the crystal is given in Table 1.

The ex situ surface enhanced Raman spectroscopy (SERS) spectra of the modified Au surface were acquired by using a Renishaw Raman Imaging Microscope System 3000 equipped with a CCD (charge coupled device) detector and an Olympus (BTH2) with a 50× objective to focus the laser beam on the sample in a backscattering configuration. As exciting radiation, λ_0, the 632.8 nm line from a He–Ne (Spectra-Physics) laser, was used.

2.5. Electrochemical behavior of NO

The solutions containing NO were prepared according to previously procedure described in the literature [27,38,39]. For preparation of NO diluted solutions, deoxygenated 0.2 mol L^{-1} Na_2SO_4 solution was placed in the electrochemical cell and aliquots of the saturated NO solution were added with a Hamilton gas-tight syringe. The applicability of these modified electrodes, as sensor for NO was assessed in 0.2 mol L^{-1} Na_2SO_4 solution as supporting electrolyte by square wave voltammetry technique (SWV) using the following parameters: frequency of pulse potential (f) of 100 s^{-1}, pulse amplitude (a) of 50 mV and scan increment (ΔE_s) of 2 mV. Analytical curves were constructed for both Au and Au/trans-[Fe(cyclam)(NCS)$_2$]$^+$ electrodes adding aliquots from stock NO solution in the electrochemical cell in the concentration range of 2.85×10^{-6} mol L^{-1} to 2.75×10^{-5} mol L^{-1}. In order to verify the applicability of this modified electrode as sensor for NO detection, the effect of possible interferences such as serotonin dopamine and nitrite was studied. All measurements were taken in triplicate.

2.6. Monte Carlo simulations

Monte Carlo simulations were performed in order to model the experimental data, since this method helps to find the most stable adsorption sites on surfaces through finding the low-energy adsorption sites on substrates or to investigate the preferential adsorption of mixtures of adsorbed components. In order to find structures at points of minimum energy, it was performed the conformational analysis of the structures by DMOL^3 software using the functional GGA (Generalized Gradient Approximation), derived from density functional theory (DFT), with the specific functional BLYP/DNP 3.5. The convergence energy adopted was 10^{-5} Ha, the maximum force and displacement was 2×10^{-3} Ha/Å and 5×10^{-3} Å respectively. The computational tools package materials studio 5.0 was used for the Monte Carlo calculations. The Au surface was modeled based on its unit cell and with its preferred Müller plane (1 1 1) [40]. In addition, the periodic structure was built using the tools available in the materials studio for building crystals and surfaces. It was used 5 cycles of heating with 100,000 steps each interaction and room temperature was applied in the simulation. The quality ultrafine was used in the calculations, implying that the parameters used were 2×10^{-5} kcal mol^{-1} variation of energy, 10^{-3} kcal mol^{-1} Å^{-1} for maximum force and range of 1×10^{-5} Å for maximum displacement in the Coordinates Cartesian. The force field used to represent the interactions of bonded and no bonded systems was the Universal [41]. For the complex and for the NO molecules and for the Au surface, the charges were set by the adopted force field. This computational study aims to find low-energy adsorption sites to investigate the preferential adsorption of NO molecules on gold surface and modified gold surface. The interactions of NO molecules with gold surface and complex adsorbed on the gold surface were carried out in a simulation box (1.73 × 1.73 nm × 2.5 nm) with periodic boundary conditions. No structure was assumed to be constant during the simulation. For the computational calculations, the amount of NO molecules ranged from 1 to 10 to represent the increase of NO concentration in the solution in order to correlate the data obtained computationally with the experimental analytical curves.

3. Results and discussion

3.1. Characterization of the synthesized complex

The thiocyanate ion has been widely studied by infrared spectroscopy, which provides a means of establishing the bonding mode. In the tetrahedral or octahedral compounds, only three vibrational modes are expected for CNS in the near infrared region. These can be assigned approximately as C—N and C—S stretches, and NCS deformation.

The C—S stretching frequencies near 700 cm^{-1} are taken as indicative of S-bonding, while those near 800–830 cm^{-1} indicate N-bonding. The C—N stretching frequency shifts on coordination

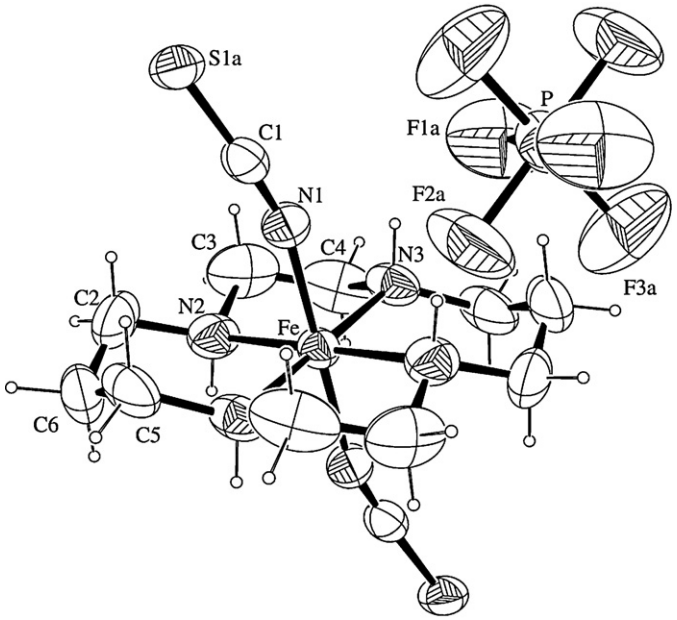

Fig. 1. ORTEP view of the complex *trans*-[Fe(cyclam)$(NCS)_2$](PF_6).

and has been considered diagnostic. N-bonding generally leads to a little change or to a decrease below the free-ion value (2053 cm^{-1} in KCNS) while S-bonding results in an increase to near 2100 cm^{-1}. A third criterion is based on the NCS deformation mode. A single and sharp band near 480 cm^{-1} is taken as indicative of N-bonding, while S-bonding is suggested by several bands of low intensity near 420 cm^{-1} [42].

The infrared spectrum of the title complex showed peaks at 483, 808 and 2059 cm^{-1} that are characteristic of δNCS deformation mode, νC—S stretching and νC—N stretching frequency, respectively, suggesting the N-bonding between thiocyanate and metal ion, which was confirmed by X-ray diffraction studies.

The ORTEP projection derived from X-ray analyses is displayed in Fig. 1, while the selected bond lengths and bond angles can be seen in Table 2. Fig. 1 shows that the structure of the synthesized complex consist of the iron metal centered in the cyclam ring and that it is coordinated to the four macrocyclic nitrogen atoms with distances of 1.980(3) Å and 1.997(2) Å. In addition, the geometry that best describes the synthesized complex is the distorted octahedron with the thiocyanate groups bound to the iron in the *trans* orientation, with a Fe-N(1)-C(1) bond angle of 162.4° and Fe-N(1) bond length of 1.899 Å, which are comparable to the angle and distance (171.7° and 1.896 Å) found in [Fe(cyclam)$(NCS)_2$]$(TCNQ)_2$

Table 2
Selected bond lengths [Å] and bond angles [°] for *trans*-[Fe(cyclam)$(NCS)_2$](PF_6).

Bond lengths (Å)			
Fe–N(1)	1.899(3)	N(1)–C(1)	1.162(5)
Fe–N(3)	1.980(3)	N(2)–C(3)	1.457(6)
Fe–N(2)	1.997(3)	N(2)–C(2)	1.489(6)
S(1A)–C(1)	1.626(11)	N(3)–C(5)	1.460(6)
S(1B)–C(1)	1.593(17)	N(3)–C(4)	1.476(6)
Fe–N(1)	1.899(3)	N(1)–C(1)	1.162(5)
Bond angles (°)			
$N(1)^i$–Fe–N(1)	180.00(1)	C(5)–N(3)–Fe	119.7(3)
N(1)–Fe–N(3)	89.98(13)	C(4)–N(3)–Fe	107.8(3)
N(1)–Fe–N(2)	90.51(14)	N(1)–C(1)–S(1B)	172.0(7)
N(3)–Fe–N(2)	85.63(15)	N(1)–C(1)–S(1A)	174.2(6)
C(1)–N(1)–Fe	162.4(3)	S(1B)–C(1)–S(1A)	12.5(11)
C(3)–N(2)–C(2)	113.8(4)	N(2)–C(2)–C(6)	112.2(4)
C(3)–N(2)–Fe	107.4(3)	N(2)–C(3)–C(4)	108.4(4)
C(2)–N(2)–Fe	117.6(3)	N(3)–C(4)–C(3)	108.0(4)
C(5)–N(3)–C(4)	11209(4)		

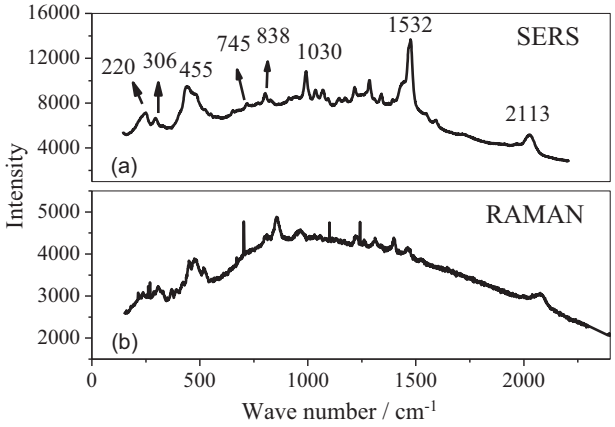

Fig. 2. (a) SERS spectrum for the gold electrode modified after 20 min of immersion in 0.2 mol L^{-1} Na_2SO_4 solution containing 0.01 mol L^{-1} *trans*-[Fe(cyclam)$(NCS)_2$](PF_6) complex. (b) Raman spectrum of the *trans*-Fe [(cyclam)$(NCS)_2$](PF_6) complex.

[43]. The presence of the PF_6^- ion disordered gives the correct charge balance for the structure. This requires that iron atom is present in the Fe^{3+} oxidation state.

The C(1)—N(1) and C(1)—S(1a) bond lengths of the thiocyanate group are 1.162 Å and 1.626, respectively, and they are similar for those observed for other thiocyanate complex [43,44]. These bound lengths are not expected for C≡N and C—S bound and a previous report, published in the literature [44], explained this fact as due to the contribution of the two below resonance structure for the thiocyanate metal complexes, as shown.

3.2. Characterization of the modified electrode

In order to have experimental evidences of the presence of the complex on the gold surface and also to model the adsorption of the complex on gold surface, SERS spectrum and cyclic voltammograms in the supporting electrolyte were obtained for freshly prepared *trans*-[Fe(cyclam)$(NCS)_2$]$^+$ layer deposited on gold electrode after 20 min of immersion of the electrode in the modifier solution.

The obtained SERS spectrum of the film adsorbed on the gold surface and the Raman spectrum of the *trans*-Fe[(cyclam)$(NCS)_2$](PF_6) complex are displayed in Fig. 2. For the SERS spectrum, the band around 220 cm^{-1} is assigned to the surface-adsorbate Au—S stretching vibration [45–51], and that one located around 306 cm^{-1} is associated to the metal-thiocyanate (N—Fe) stretching frequencies [51], the band around 455 cm^{-1} is attributed to the N—C—S stretching, little band at 745 cm^{-1} is assigned to the C—S stretching vibrations [45–51], the peak observed at 800 cm^{-1} is typical for N-bound metal-thiocyanate complex (N—Fe) [51], bands observed between 1030 cm^{-1} and 1532 cm^{-1} are related to the internal vibration mode of the complex molecule [52] and, finally, the peak located at 2113 cm^{-1} is assigned to the C—N stretching mode [45–51] of the thiocyanate ligand. Thus, the band observed about 220 cm^{-1} suggests that the complex is bound on the gold surface by the sulfur atom and that the nitrogen is bounded to the transition-metal cation. In addition, it can be observed in the SERS spectrum that the bands related to the vibration mode of the internal molecule (1030–1532 cm^{-1}) are intensified in relation to the Raman spectrum, indicating that the *trans*-[Fe (cyclam)$(NCS)_2$]$^+$ ion complex is adsorbed on the surface of gold after the immersion time of 20 min.

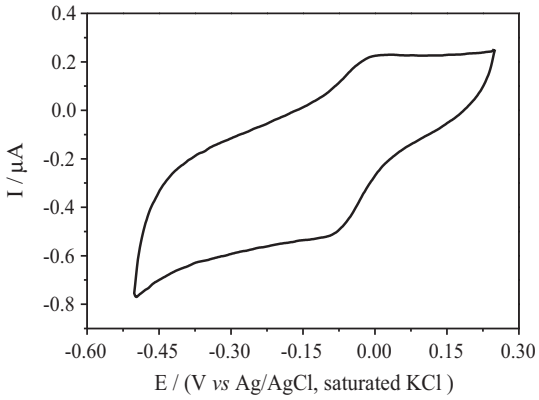

Fig. 3. Cyclic voltammograms of the Au/*trans*-[Fe(cyclam)(NCS)$_2$]$^+$ electrodes obtained at 0.1 V s^{-1} in 0.2 mol L^{-1} Na_2SO_4 solution.

The cyclic voltammetric profile of the modified electrode in the supporting electrolyte is displayed in Fig. 3. This plot shows a broad cathodic peak around −0.1 V and a broad anodic peak around 0.0 V. This couple of peak is characteristic of the $Fe^{III/II}$ redox couple. Thus, SERS and cyclic voltammetry results are experimental evidences of the successful modification of the gold surface by the *trans*-[Fe(cyclam)(NCS)$_2$]$^+$ species.

3.3. Electrochemical and Monte Carlo studies

Typical cyclic voltammograms of the NO on both unmodified and modified gold electrodes displayed an irreversible anodic current peak around 0.85 V, as shown in Fig. 4a. This peak is related to the one electron transfer reaction related with the oxidation of NO according to Eq. (1) [28].

$$NO \rightarrow NO^+ + e^- \quad (1)$$

Mori and Berttoti [28] pointed out that the nitrosium cation NO^+ is stable at high proton concentration and that the nitrous acid is the prevalent species in neutral medium according to equation 2

$$HNO_2 + H^+ = NO^+ + H_2O, \quad k = 7 \times 10^{-5} \quad (2)$$

Finally, according to these authors, the overall reaction of the NO oxidation on the Au and Au/trans-[Fe(cyclam)(NCS)$_2$]$^+$ electrodes in 0.2 mol dm^{-3} Na_2SO_4 solution is expressed by equation (3) [28].

$$NO + H_2O = HNO_2 + H^+ + e^- \quad (3)$$

It can be observed in Fig. 4b that the peak currents (I_p) for the NO oxidation on the modified electrodes are higher than that for the unmodified electrode, showing that the modification of the gold electrode with *trans*-[Fe(cyclam)(NCS)$_2$]$^+$ species leads to an increase in the rate of the electron transfer reaction at the electrode-solution interface. These results are in close agreement with those reported in the literature for gold electrodes modified with Ru-based complexes: *trans*-[Ru(NH$_3$)$_4$(SO$_4$)^{4}pic]$^+$ [27] and *trans*-[Ru(NH$_3$)$_4$(Ist)(SO$_4$)]$^+$ [28].

Furthermore, Fig. 4b also shows that I_p rises linearly with the modification time of the gold electrode until 20 min of modification, remaining approximately constant for higher modification time. The observed linear dependence of the I_p with the modification time can be explained as due to the increase of the surface coverage with the immersion time of the gold electrode in the modifier solution. The independence of the I_p with the modification time after 20 min of modification suggests that the maximum surface coverage of the gold surface with complex species is achieved with 20 min of immersion of the gold electrode in the modifier solution. From these results, in order to evaluate the Au/*trans*-[Fe(cyclam)(NCS)$_2$]$^+$ electrode as electrochemical sensor for NO, it

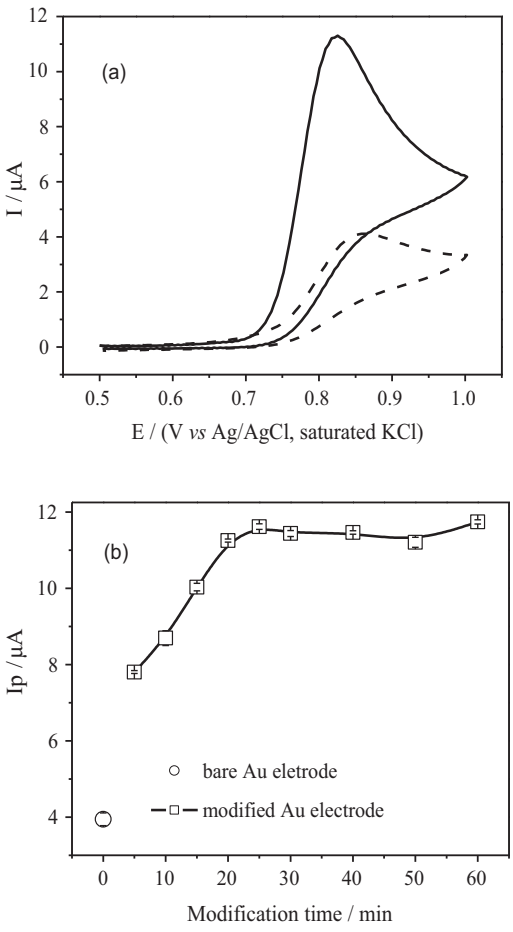

Fig. 4. (a) Cyclic voltammograms obtained at 0.1 V s^{-1} in 0.2 mol L^{-1} Na_2SO_4 solution and containing 1.14 × 10^{-5} mol L^{-1} NO for the bare Au electrode (dashed line) and for modified Au electrode after immersion in modifier solution for 20 min (solid line); (b) influence of the modification time on the peak current of the NO oxidation.

was selected the modification time of 20 min. Finally, the I_p was linear with the square root of the scan rate, showing that the NO oxidation is controlled by diffusion on Au/*trans*-[Fe(cyclam)(NCS)$_2$]$^+$ electrodes. These results suggest that for the electrochemical oxidation of NO, the *trans*-[Fe(cyclam)(NCS)$_2$]$^+$ complex act as a simple coating without the participation of Fe^{2+}/Fe^{3+} couple.

The analytical curves for Au and Au/*trans*-[Fe(cyclam)(NCS)$_2$]$^+$ electrodes, derived from the square wave voltammograms, are presented in Fig. 5. Initially, a good linear relationship between the peak current and the NO concentration is observed for both electrodes, being the slope of the analytical curve of the modified electrode higher than that presented for the analytical curve of the unmodified electrode. These results indicate that the modification of the gold surface with *trans*-[Fe(cyclam)(NCS)$_2$]$^+$ species improves the sensitivity for anlytical purposes of NO detection.

Table 3 presents the analytical parameters derived from the analytical curves for the NO determination on Au and Au/*trans*-[Fe(cyclam)(NCS)$_2$]$^+$ electrodes using the SWV. These include the linearity range (LR), analytical curve equations, correlation coefficients (R; determined by the degree of linearity for the correlation between NO concentration and peak currents), detection limits (DL), quantification limits (QL). All data shown in this table were obtained in triplicate, and the results reported here represent the average of the values obtained. The values of DL and QL were calculated as recommended by IUPAC [53].

As can be observed in Table 3, the intercepts of the analytical curves were negative. Therefore, an evaluation of the presence of

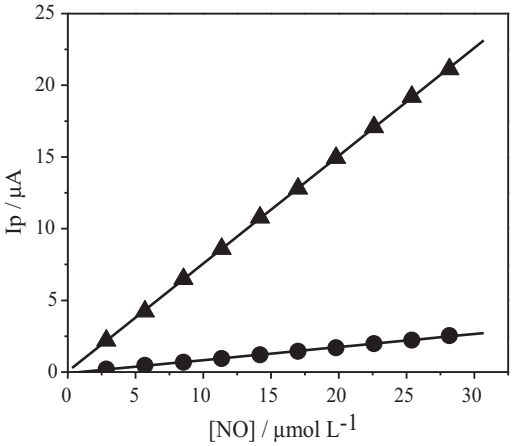

Fig. 5. Analytical curves for Au and Au/*trans*-[Fe(cyclam)(NCS)$_2$]$^+$ electrodes obtained in 0.2 mol L^{-1} Na_2SO_4 solution containing NO in concentration range of 2.85×10^{-6} mol L^{-1} to 2.82×10^{-5} mol L^{-1} and using SWV with the following parameters: $f = 100\ s^{-1}$, $a = 50$ mV and $\Delta E_s = 2$ mV.

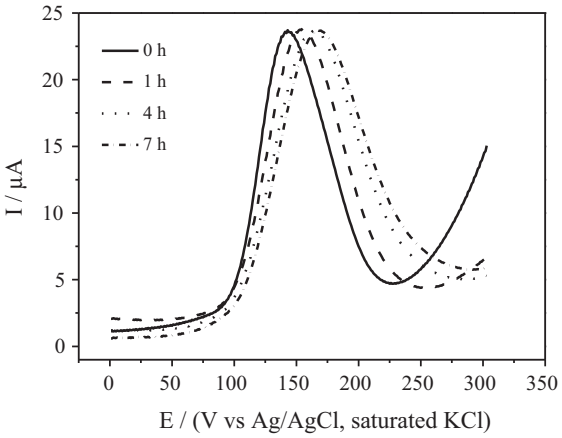

Fig. 6. Influence of the aging time of the film on the electrochemical response of the NO on the Au/*trans*-[Fe(cyclam)(NCS)$_2$]$^+$ electrode.

random errors was performed by a significance test in order to determine if the difference between the interception obtained in these analytical curves and the standard values were originated from random error [54]. The *t*-test was used, according to Eq. (4), where $\bar{x}$ is the average obtained from interception values, μ is the standard value expected in the case of the interception being zero, *n* is the number of determinations, and s is the standard deviation of the current responses.

$$t = (\bar{x} - \mu)\frac{\sqrt{n}}{s} \quad (4)$$

For a 95% confidence level, the calculated t values were 1.95 and 0.41 for Au and for Au/*trans*-[Fe(cyclam)(NCS)$_2$]$^+$ electrodes, respectively. As the critical value of *t* for *n* = 3 is 4.30, statistically, the value of the linear coefficient is zero. In addition, Table 3 shows that DL and QL obtained for Au/*trans*-[Fe(cyclam)(NCS)$_2$]$^+$ electrode is about one order lesser than the corresponding values obtained for the Au electrode. The DL value of the Au/*trans*-[Fe(cyclam)(NCS)$_2$]$^+$ electrode is very close to those presented by the Au/*trans*-[Ru(NH$_3$)$_4$(Ist)(SO$_4$)]$^+$ electrode [28] and for others systems such Pt ultramicroelectrodes coated with films of metal tetraaminophthalocyanines (MTAPc, M=Co, Ni, Cu) [55], Au ultramicroelectrodes modified with ironphthalocyanine [56], glassy carbon electrode modified with multiwall carbon nanotube [57], with multiwall carbon nanotube/chotosan/NiO [58] and with fullerene [59], and for carbon fiber ultramicroelectrode coated multiwall carbon nanotube [60].

In order to assess the stability of the proposed electrode for NO detection, the peak current of the NO oxidation with the aging time of the film was evaluated and the results are shown in Fig. 6. This Fig. shows that the peak current remains approximately constant with the aging time, indicating that, even with 7 h of aging time, the trans-[Fe(cyclam)(NCS)$_2$]$^+$ complex remains on the gold surface. This good stability of the *trans*-[Fe(cyclam)(NCS)$_2$]$^+$ self-assembled layer on the gold surface is explained as due to the formation of the strong Au—S bond. Furthermore, the peak potential slightly shifts to more positive values, indicating that the overpotential of the NO oxidation on the modified electrode increases with the aging time, suggesting that the film is slightly less electrocatalyst for NO oxidation with the aging time.

Monte Carlo simulation was carried out in order to explain the better analytical sensitivity of the modified electrode for NO detection in comparison with the unmodified gold electrode. Fig. 7 presents the preferred orientation of the NO molecules interacting with the gold surface. The number of NO molecules was changing from 1 until 10 to represent the increase of the NO concentration in solution. The dashed lines observed in Fig. 7 represent the nearer interaction observed to each molecule. This Fig. shows that the increase of the number of NO molecules interacting with gold surface leads to formation of molecular clusters. This can be explained as a consequence of the adsorption of the first NO molecule on Au surface which acts as a preferential nucleation site for the adsorption of the others molecules. In addition, it can also be observed that for higher amount of NO molecules, some NO molecules tend to interact with the primary nuclei formed, suggesting that the molecular clusters is not restricted to a monolayer.

The preferential orientation of the trans-[Fe(cyclam)(NCS)$_2$]$^+$ complex on Au surface, calculated from the Monte Carlo calculation, is shown in Fig. 8. The dashed line, shown in this Fig., indicates that the sulfur atom of the trans-[Fe(cyclam)(NCS)$_2$]$^+$ complex has the nearer interaction with the Au surface with calculated interaction energy of −135.26 kcal mol^{-1}, suggesting that the adsorption of the trans-[Fe(cyclam)(NCS)$_2$]$^+$ complex on the Au surface occurs due to

Table 3
Analytical parameters obtained from the analytical curves for the determination of NO on Au and Au/*trans*-[Fe(cyclam)(NCS)$_2$]$^+$ electrodes using the SWV. LR: linearity range; R: correlation coefficient; DL: detection limit; QL: quantification limit.

Analytical parameter	Electrodes	
	Au	Au/*trans*-[Fe(cyclam)(NCS)$_2$]$^+$
LR/mol L^{-1}	From 2.85×10^{-6} to 2.82×10^{-5}	From 2.85×10^{-6} to 2.82×10^{-5}
Equation curve	$I_p = (-0.05 \pm 0.07) + (0.09 \pm 0.01)$[NO]	$I_p = (-0.11 \pm 0.17) + (0.76 \pm 0.04)$[NO]
R	0.999	0.999
DL (mol L^{-1})	8.29×10^{-7} (24.86 μg L^{-1})	5.15×10^{-8} (1.55 μg L^{-1})
QL (mol L^{-1})	2.76×10^{-6} (82.86 μg L^{-1})	1.72×10^{-7} (5.16 μg L^{-1})
t-Test	1.95	0.41

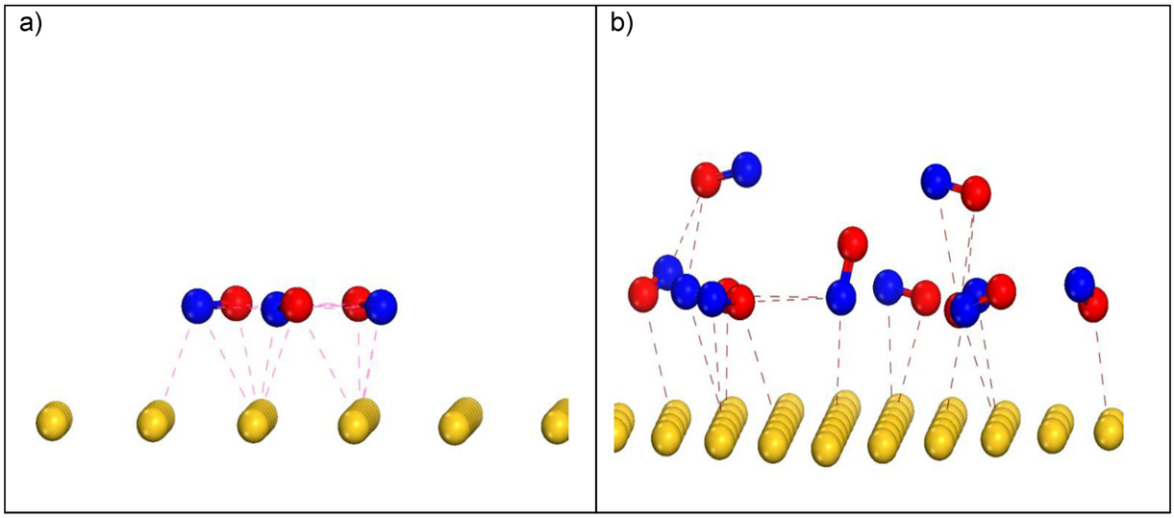

Fig. 7. Preferred orientation of the NO molecules interacting with the surface of Au for 3 NO molecules (a) and for 10 NO molecules (b). The calculations were made using Monte Carlo computational method.

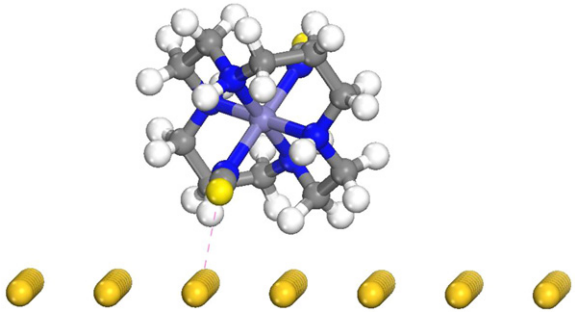

Fig. 8. Preferential orientation of the *trans*-$[Fe(cyclam)(NCS)_2]^+$ complex ion on gold surface calculated by Monte Carlo computational method.

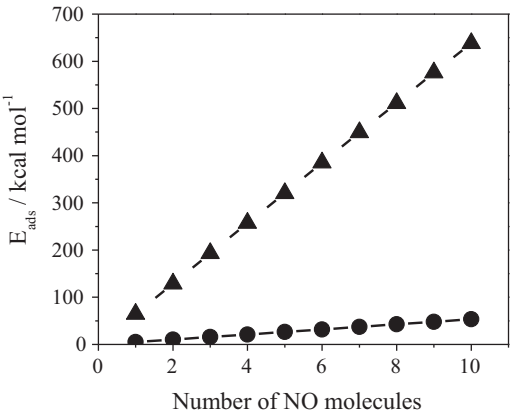

Fig. 9. Dependence of the calculated interaction energy with the number of NO molecules for Au (●) and for Au/*trans*-$[Fe(cyclam)(NCS)_2]^+$ (▲) electrodes. The calculations were made using Monte Carlo computational method.

the Au—S chemical bond. These results show that the Monte Carlo calculations for the adsorption of the trans-$[Fe(cyclam)(NCS)_2]^+$ on Au surface are in concordance with experimental evidence given by the SERS spectrum.

Fig. 9 shows that there is a good linear dependence between the calculated total interaction energy with the number of NO molecules, that the slope of the modified electrode is higher and the values of the interaction energies of the modified electrode is much more negatives than those of the unmodified electrode, which means that interaction between the NO molecule with the trans-[Fe(cyclam)(NCS)2] adsorbed molecule is much more stronger than that of the NO with the Au atom. Furthermore,

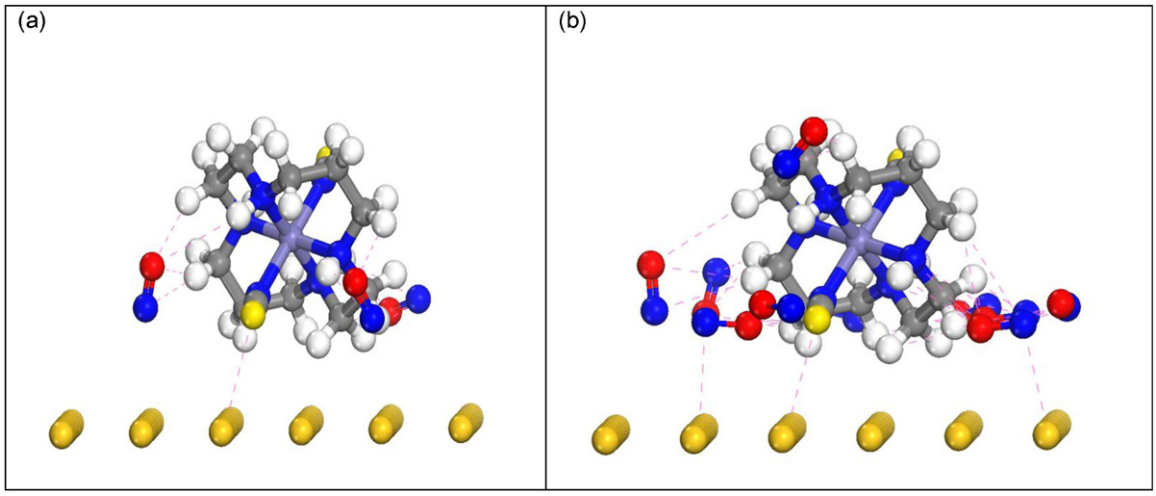

Fig. 10. Preferred orientation of the NO molecules interacting with the Au/*trans*-$[Fe(cyclam)(NCS)_2]^+$ surface for 3 NO molecule (a) and for 10 NO molecules (b). The calculations were made using Monte Carlo computational method.

a good correlation between the experimental analytical curves (Fig. 5) and the calculated values, derived from Monte Carlo simulation (Fig. 9), is observed. Therefore, from the Monte Carlo calculation, the improvement of the peak current signal observed experimentally for the modified electrode is explained as due to the stronger interaction between the NO molecules with the *trans*-[Fe(cyclam)(NCS)$_2$] adsorbed molecules.

Fig. 10 shows the increase of the number of the NO molecules interacting with the Au/*trans*-[Fe(cyclam)(NCS)$_2$]$^+$ electrode surface. It is possible to see that the NO has a larger concentration in the Fe–cyclam's neighborhood. The dashed lines indicate that the NO preferentially interacts with the hydrogen atoms of the trans-[Fe(cyclam)(NCS)$_2$]$^+$ adsorbed molecule making hydrogen bonds, and not with the Au surface. Thus, with the Monte Carlo simulation is possible to argue that the higher current response for NO oxidation presented by the Au/*trans*-[Fe(cyclam)(NCS)$_2$]$^+$ surface is due to the stronger interaction of the NO molecules with trans-[Fe(cyclam)(NCS)$_2$]$^+$ complex adsorbed on the Au surface than the interaction of NO with the bare Au surface.

In order to verify possible interferences from other biological molecules such as dopamine and serotonin in the determination of NO, the NO electrochemical oxidation on the Au/*trans*-[Fe(cyclam)(NCS)$_2$]$^+$ electrode in the presence of these two molecules was evaluated. Fig. 11 shows the square wave voltammograms for the Au/*trans*-[Fe(cyclam)(NCS)$_2$]$^+$ electrode in 0.2 M Na_2SO_4 solutions containing NO in the concentration range of 8.53×10^{-6} to 2.82×10^{-5} mol L^{-1} with 1.0×10^{-4} mol L^{-1} of dopamine (Fig. 11a) and serotonin (Fig. 11b), and in the presence of both interferents with equal concentration of 1.0×10^{-4} mol L^{-1} (Fig. 11c).

Fig. 11a shows that it is not observed a peak related to the oxidation of dopamine on Au/*trans*-[Fe(cyclam)(NCS)$_2$]$^+$ electrode in the absence of NO (dashed line). However, in the presence of NO (solid lines), a peak appears between 0.3 V and 0.40 V, being that this peak current increases and its peak potential slightly shifts for more positive values with the NO concentration. For the serotonin in the absence of NO (dashed line in Fig. 11b), an oxidation peak around 0.50 V is observed in the square wave voltammogram, while in the presence of the NO, a new peak about 0.3 V appears. Furthermore, the serotonin peak current decreases and the peak around 0.3 V becomes more evident with the increase of NO concentration. The square wave voltammogram for NO in the presence of 1.0×10^{-4} mol dm^{-3} of both interferents (Fig. 11c) shows the peaks at about 0.3 V and 0.5 V, which present similar behavior with those that shown in Fig. 11b.

Comparing the NO oxidation potential in the presence and absence of dopamine and serotonin, non significant shift in the NO oxidation potential is observed. However, the slope of the analytical curve obtained in the presence of these interferents (I_p (μA) = (0.50 ± 0.84) + (0.43 ± 0.11) [NO/mol L^{-1}]) is smaller than that obtained in the absence of these interferents. This can be explained by the fact that NO is consumed by these interferents, since it is known from the literature that NO promotes the deamination of some natural amines [61]. Thus, the results suggest that the oxidation peak current observed around 0.3 V in the square wave voltammograms present in Fig. 11 are related to the electrochemical oxidation of the deamination products of dopamine and serotonin.

It was also analyzed the nitrite interference in the NO detection using a Au/*trans*-[Fe(cyclam)(NCS)$_2$]$^+$ electrode and the related voltammograms are shown in Fig. 12. Nitrite showed an anodic

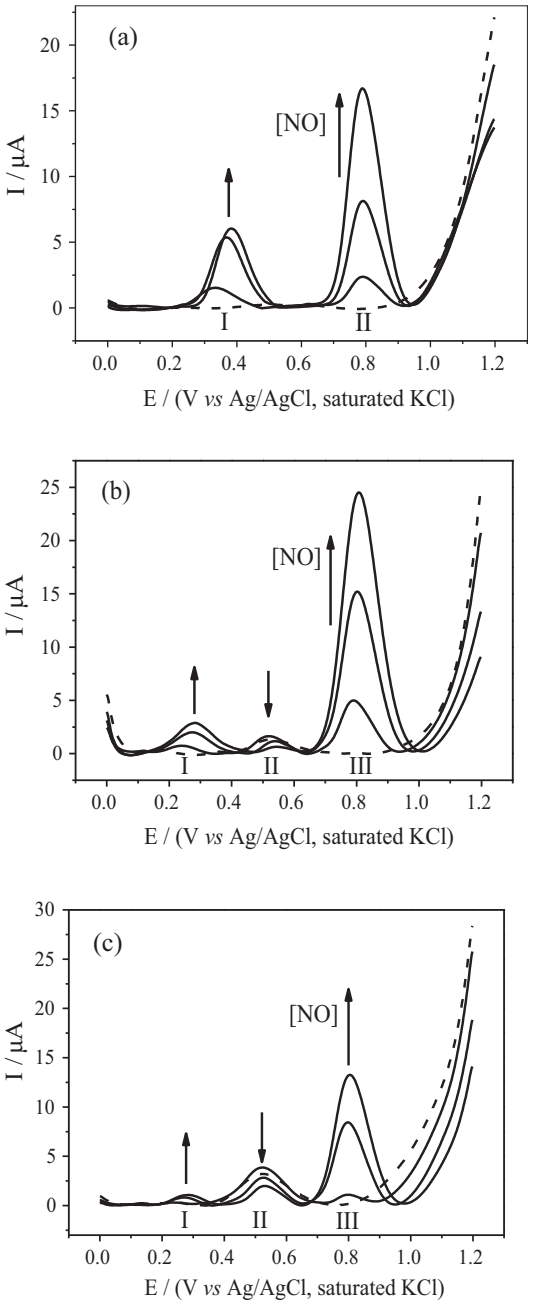

Fig. 11. Square wave voltammograms for Au/*trans*-[Fe(cyclam)(NCS)$_2$]$^+$ electrode in 0.2 mol L^{-1} Na_2SO_4 solution containing NO in concentration range of 8.53×10^{-6} mol L^{-1} to 2.82×10^{-5} mol L^{-1} and equal concentration of 1.0×10^{-4} mol L^{-1} of dopamine (a) and serotonin (b) and in the presence of both molecules (c) obtained with f = 100 s^{-1}, a = 50 mV and ΔEs = 2 mV.

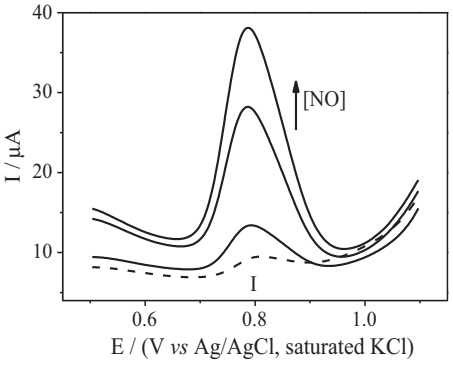

Fig. 12. Square wave voltammograms for Au/*trans*-[Fe(cyclam)(NCS)$_2$]$^+$ electrode in 0.2 mol L^{-1} Na_2SO_4 solution containing NO in concentration range of 2.85×10^{-6} mol L^{-1} to 2.26×10^{-5} mol L^{-1} and 1.0×10^{-4} mol L^{-1} NO_2^- obtained with f = 100 s^{-1}, a = 50 mV and ΔE_s = 2 mV.

peak around 0.80 V, the same oxidation potential of NO. This result justifies the fact that the slope of analytical curve for the oxidation of NO obtained in the presence of NO_2^- (I_p (μA) = (2.56 ± 0.22) + (1.04 ± 0.03) [NO/mol L^{-1}]) is greater than that obtained in the absence of this interferent, confirming that this specie interferes in the determination of NO. This behavior is in agreement with results reported in the literature [62]. Finally, a comparison of the sensitivity values shows that the response for the dopamine and serotonin is less significant than the responses for nitrite.

4. Conclusions

The synthesized complex has distorted octahedron geometry with the thiocyanate groups bonded to the iron ion by the nitrogen atom and in the *trans* orientation. *Trans*-$[Fe(cyclam)(NCS)_2]^+$ complex ion was successful self-assembled on gold electrode and the by SERS spectrum and Monte Carlo calculation support that the complex ion is adsorbed on Au surface by the Au—S bond. The current for NO oxidation on the modified electrode is higher than that presented by the bare Au electrode and a good correlation is presented by the experimental analytical curve and the calculated Monte Carlo interaction energy versus amount NO molecules plot. The Monte Carlo simulation indicates that the higher current response for NO oxidation on the Au/*trans*-$[Fe(cyclam)(NCS)_2]^+$ surface is due to the stronger interaction of NO molecules with trans-$[Fe(cyclam)(NCS)_2]^+$ complex adsorbed on the Au surface than the interaction of NO with the bare Au surface. The theoretical analyses also reveal that NO molecules cluster on bare Au surface. Dopamine, serotonin and nitrite are interferents for the detection of NO with dopamine and serotonin is less significant interferents than the nitrite. The proposed modified electrode present good electrochemical stability, detection limit and quantification limit of 5.15×10^{-8} mol L^{-1} and 1.72×10^{-7}, respectively, which were about one order of magnitude lesser than the corresponding values obtained for the bare Au electrode. The results indicate that the proposed electrode has potential to be applied as a sensor for NO detection.

Acknowledgements

The authors gratefully acknowledge funding provided by the following Brazilian agencies: CNPq-INCT (Proc. 573925/2008-9 and 573548/2008-0), CAPES (Procad NF 2424/2008) and FINEP. Pedro de Lima-Neto (proc. 301746/2011-7), Luis G.F. Lopes (proc. 301478/2008-2), Jackson R. Sousa (proc. 308354/2011-7) and Vanessa N. Santos (proc. 551663/2010-3) thank CNPq for their grants. Acknowledgment is also made to Prof. M. L. A. Temperini (Instituto de Quimica-USP, Brazil) for the SERS data.

References

[1] S. Moncada, M. Feelisch, R. Busse, E.A. Higgs (Eds.), The Biology of Nitric Oxide 3: Physiological and Clinical Aspects, Portland Press, London, 1994.
[2] B.A. Weissman, N. Allon, S. Shapira (Eds.), Biochemical, Pharmacological and Clinic Aspects of Nitric Oxide, Plenum Press, USA and Canada, 1995.
[3] C.N. Hall, J. Garthwaite, What is the real physiological NO concentration in vivo? Nitric Oxide 15 (2009) 92.
[4] Y. Wang, S. Hu, A novel nitric oxide biosensor based on electropolymerization poly(toluidine blue) film electrode and its application to nitric oxide released in liver homogenate, Biosensors and Bioelectronics 22 (2006) 10.
[5] F. Bedioui, S. Trevin, J. Devynck, Chemically modified microelectrodes designed for the electrochemical determination of nitric oxide in biological systems, Electroanalysis 8 (1996) 1085.
[6] S. Miserere, S. Ledru, N. Ruillé, S. Griveau, M. Boujtita, F. Bedioui, Biocompatible carbon-based screen-printed electrodes for the electrochemical detection of nitric oxide, Electrochemistry Communications 8 (2006) 238.
[7] F. Bedioui, D. Quinton, S. Griveau, T. Nyokong, Designing molecular materials and strategies for the electrochemical detection of nitric oxide superoxide and peroxynitrite in Physical Chemistry, Chemical Physics 12 (2010) 9976.
[8] F. Bedioui, S. Trevin, J. Devynck, F. Lantoine, A. Brunet, M.A. Devynck, Elaboration and use of nickel planar macrocyclic complex-based sensors for the direct electrochemical measurement of nitric oxide in biological media, Biosensors and Bioelectronics 12 (1997) 205.
[9] M. Pontié, H. Lecture, F. Bedioui, Improvement in the performance of a nickel complex-based electrochemical sensor for the detection of nitric oxide in solution, Sensors and Actuators B 56 (1999) 1.
[10] M. Pontié, C. Gobin, T. Pauporté, F. Bedioui, J. Devynck, Electrochemical nitric oxide microsensors: sensitivity and selectivity characterisation, Analytica Chimica Acta 411 (2000) 175.
[11] T. Nyokong, S.L. Vilakazi, Phthalocyanines and related complexes as electrocatalysts for the detection of nitric oxide, Talanta 61 (2003) 27.
[12] E. Casero, J. Losada, F. Pariente, E. Lorenzo, Modified electrode approaches for nitric oxide sensing, Talanta 61 (2003) 61.
[13] J. Oni, N. Diab, S. Reiter, W. Schuhmann, Metallophthalocyanine-modified glassy carbon electrodes: effects of film formation conditions on electrocatalytic activity towards the oxidation of nitric oxide, Sensors and Actuators B 105 (2005) 208.
[14] I.K. Kim, H.T. Chung, G.S. Oh, H.O. Bae, S.H. Kim, H.J. Chun, Integrated gold-disk microelectrode modified with iron(II)-phthalocyanine for nitric oxide detection in macrophages, Microchemical Journal 80 (2005) 219.
[15] S.L. Vilakazi, T. Nyokong, Voltammetric determination of nitric oxide on cobalt phthalocyanine modified microelectrodes, Journal of Electroanalytical Chemistry 512 (2011) 56.
[16] A.K.M. Holanda, F.O.N. Silva, J.R. Sousa, I.C.N. Diógenes, I.M.M. Carvalho, I.S. Moreira, M.J. Clarke, L.G.F. Lopes, Photochemical NO release from nitrosyl RuII complexes with C-bound imidazoles, Inorganica Chimica Acta 361 (2008) 2929.
[17] F.O.N. Silva, S.X.B. Araújo, A.K.M. Holanda, E. Meyer, F.A.M. Sales, I.C.N. Diógenes, I.M.M. Carvalho, I.S. Moreira, L.G.F. Lopes, Synthesis, Characterization, and NO Release Study of the cis- and trans-$[Ru(Bpy)_2(SO_3)(NO)]^+$ Complexes, European Journal of Inorganic Chemistry 2006 (2006) 2020.
[18] P.G.Z. Benini, B.R. Mcgarvey, D.W. Franco, Functionalization of PAMAM dendrimers with $[Ru^{III}(edta)(H_2O)]$, Nitric Oxide 19 (2008) 245.
[19] L.G.F. Lopes, A. Wieraszko, Y. El-Sherif, M.J. Clarke, The trans-labilization of nitric oxide in RuII complexes by C-bound imidazoles, Inorganica Chimica Acta 312 (2001) 15.
[20] A. Wieraszko, M.J. Clarke, D.R. Lang, L.G.F. Lopes, D.W. Franco, The influence of NO-containing ruthenium complexes on mouse hippocampal evoked potentials in vitro, Life Sciences 68 (2001) 1535.
[21] A.K.M. Holanda, D.L. Pontes, I.C.N. Diógenes, I.S. Moreira, L.G.F. Lopes, NO release from trans-$[Ru(NH_3)4L(NO)]^{3+}$ complexes upon reduction (L = 1-methylimidazole or benzoimidazole), Transition Metal Chemistry 29 (2004) 430.
[22] F.O.N. Silva, M.C.L. Cândido, A.K.M. Holanda, I.C.N. Diógenes, E.H.S. Sousa, L.G.F. Lopes, Mechanism and biological implications of the NO release of cis-$[Ru(bpy)_2L(NO)]^{n+}$ complexes: A key role of physiological thiols, Journal of Inorganic Biochemistry 105 (2011) 624.
[23] F.O.N. Silva, E.C.C. Gomes, T.S. Francisco, A.K.M. Holanda, I.C.N. Diógenes, E.H.S. Sousa, L.G.F. Lopes, E. Longhinotti, NO donors cis-$Ru(bpy)_2(L)NO]^{3+}$ and $[Fe(CN)_4(L)NO]^-$ complexes immobilized on modified mesoporous silica spheres, Polyhedron 29 (2010) 3349.
[24] A.K.M. Holanda, F.O.N. Silva, I.M.M. Carvalho, A.A. Batista, J. Ellena, E.E. Castelano, I.S. Moreira, L.G.F. Lopes, Crystal structure, electrochemical and photochemical studies of the trans-$[Fe(cyclam)(NO)Cl]Cl_2$ Complex (cyclam = 1,4,8,11-tetraazacyclotetradecane), Polyhedron 26 (2007) 4653.
[25] L.G.F. Lopes, E.E. Castellano, A.G. Ferreira, C.U. Davanzo, M.J. Clarke, D.W. Franco, trans-$[Ru(NH_3)_4P(OEt)_3NO]X_3$ (X = PF_6^-, CF_3COO^-): modulation of the release of NO by the trans-effect, Inorganica Chimica Acta 358 (2005) 2883.
[26] L.G.F. Lopes, E.H.S. Sousa, J.C.V. Miranda, C.P. Oliveira, I.M.M. Carvalho, A.A. Batista, J. Ellena, E.E. Castellano, O.R. Nascimento, I.S. Moreira, Crystal structure, electrochemical and spectroscopic properties of the trans-$K\{[FeCl(NO^0)(cyclam)].[FeCl(NO)^+(cyclam)]_2\}(PF_6)_6$ complex, Journal of the Chemical Society-Dalton Transactions 9 (2002) 1903.
[27] V. Mori, J.C. Toledo, H.A.S. Silva, D.W. Franco, M. Bertotti, Anodic oxidation of free nitric oxide at gold electrodes modified by a film of trans-$[Ru(III)(NH_3)_4(SO_4)4pic]$ and molybdenum oxide, Journal of Electroanalytical Chemistry 547 (2003) 9.
[28] V.N. Santos, M.F. Cabral, J.S. Ferreira, A.K.M. Holanda, S.A.S. Machado, J.R. Sousa, L.G.F. Lopes, A.N. Correia, P. de Lima-Neto, Study of a gold electrode modified by trans-$[Ru(NH_3)_4(Ist)SO_4]^+$ to produce an electrochemical sensor for nitric oxide, Electrochimica Acta 56 (2011) 5686.
[29] N. Metropolis, A.W. Rosenbluth, M.N. Rosenbluth, A.H. Teller, E. Teller, Equation of state calculations by fast computing machines, Journal of Chemical Physics 21 (1953) 1087.
[30] B.J. Alder, T.E. Wainwright, Phase transition for a hard sphere system, Journal of Chemical Physics 27 (1957) 1208.
[31] R. Guilard, O. Siri, A. Tabard, G. Broeker, P. Richard, D.J. Nurco, K.M. Smith, One-pot synthesis, physicochemical characterization and crystal structures of cis- and trans-(1,4,8,11-tetraazacyclotetradecane)- dichloroiron(III) complexes, Journal of the Chemical Society – Dalton Transactions 19 (1997) 3459.
[32] Enraf-Nonius *COLLECT*, B. V. Nonius, Delft, The Netherlands, 1997–2000.
[33] Z. Otwinowski, W. Minor, Processing of X-ray diffraction data collected in oscillation mode, Method Enzymology 276 (1997) 307.
[34] P. Coppens, L. Leiserowitz, D. Rabinovich, Calculation of absorption corrections for camera and diffractometer, Acta Crystallographica 18 (1965) 1035.

[35] G.M. Sheldrick, SHELXS-97: Program for Crystal Structure Resolution, University of Göttingen, Germany, 1997.
[36] G.M. Sheldrick, SHELXL-97: Program for Crystal Structures Analysis, University of Göttingen, Germany, 1997.
[37] L.J. Farrugia, ORTEP-3 for Windows - a version of ORTEP-III with a Graphical User Interface (GUI), Journal of Applied Crystallography 30 (1997) 565.
[38] L. Kosminsky, V. Mori, M. Bertotti, Electrochemical studies on the oxidation of nitric oxide (NO) at glassy carbon electrodes modified by molybdenum oxides, Journal of Electroanalytical Chemistry 499 (2001) 176.
[39] V. Mori, M. Bertotti, Nitric oxide solutions: standardisation by chronoamperometry using a platinum disc microelectrode, Analyst 125 (2000) 1629.
[40] G. Hong, H. Heinz, R.R. Naik, B.L. Farmer, R. Pachter, Toward understanding amino acid adsorption at metallic interfaces: a density functional theory study, Applied Materials and Interfaces 1 (2009) 388.
[41] A.K. Rappe, C.J. Casewit, K.S. Colwell, W.A. Goddard, W.M. Skiff, Application of a Universal Force Field to Main Group Compounds, Journal of the American Chemical Society 114 (1992) 10024.
[42] R.A. Bailey, S.L. Kozac, T.W. Michelsen, W.N. Mills, Infrared spectra of complexes of the thiocyanate and related ions, Coordination Chemistry Reviews (1971) 407.
[43] L. Ballester, A. Gutiérrez, F. Perpiñán, S. Rico, M.T. Azcondo, C. Bellitto, Magnetic behavior and crystal structure of $[Fe(cyclam)(NCS)_2](TCNQ)_2$: an unusual one-dimensional $(TCNQ)^{2-}$ radical-ion system, Inorganic Chemistry 38 (1999) 4430.
[44] R.M.C. Brito, A.A. Batista, J. Ellena, E.E. Castellano, I.C.N. Diógenes, L.G.F. Lopes, J.R. Sousa, I.S. Moreira, Synthesis, characterization and crystal structure of a novel thiocyanate–ruthenium(II) complex, Inorganic Chemistry Communications 10 (2007) 1515.
[45] D.S. Corrigan, J.K. Foley, P. Gao, S. Pons, M.J. Weaver, Comparisons between surface-enhanced Raman and surface infrared spectroscopies for strongly perturbed adsorbates: thiocyanate at gold electrodes, Langmuir 1 (1985) 616.
[46] P. Gao, M.J. Weaver, Metal-adsorbate vibrational frequencies as a probe of surface bonding: halides and pseudohalldes at gold electrodes, Journal of Physical Chemistry 90 (1986) 4057.
[47] D.S. Corrigan, J.K. Foley, P. Gao, S. Pons, M.J. Weaver, Comparisons between surface infrared and surface-enhanced Raman spectroscopies: band frequencies, bandwidths, and Selection Rules for pseudohalide and related adsorbates at gold and silver electrodes, Langmuir 2 (1986) 744.
[48] M. Bron, R. Holze, The adsorption of thiocyanate ions at gold electrodes from an alkaline electrolyte solution: a combined in situ infrared and Raman spectroscopic study, Electrochimica Acta 45 (1999) 1121.
[49] X. Li, A.A. Gewirth, Potential-dependent reorientation of thiocyanate on Au electrodes, Journal of the American Chemical Society 125 (2003) 11674.
[50] H. Kang, J. Noh, E. Ganbold, D. Uuriintuya, M. Gong, J.J. Oh, S. Joo, Adsorption changes of cyclohexyl isothiocyanate on gold surfaces, Journal of Colloid and Interface Science 336 (2009) 648.
[51] H. Luo, M.J. Weaver, Surface-enhanced Raman scattering as a versatile vibrational probe of transition-metal interfaces: thiocyanate coordination modes on platinum-group versus coinage-metal electrodes, Langmuir 15 (1999) 8743.
[52] J. Bukowska, G. Roslonek, J. Taraszewska, In-situ surface-enhanced Raman spectroscopic study of gold electrodes modified with nickel tetraazamacrocyclic complexes, Journal of Electroanalytical Chemistry 403 (1996) 47.
[53] J. Mocak, A.M. Bond, S. Mitchel, G. Scollary, A statistical overview of standard (IUPAC and ACS) and new procedures for determining the limits of detection and quantification: application to voltammetric and stripping techniques, Pure and Applied Chemistry 69 (1997) 297.
[54] J.N. Miller, J.C. Miller, Statistics and Chemometrics for Analytical Chemistry, 5th ed., Pearson Prentice Hall, United Kingdom, 2005.
[55] J. Jin, T. Miwa, L. Mao, H. Tu, L. Jin, Determination of nitric oxide with ultramicrosensors based on electropolymerized films of metal tetraaminophthalocyanines, Talanta 48 (1999) 1005.
[56] I.K.J. Kim, H.T. Chung, G.S. Oh, H.O. Bae, S.H. Kim, H.J. Chun, Integrated gold-disk microelectrode modified with iron(II)-phthalocyanine for nitric oxide detection in macrophages, Microchemical Journal 80 (2005) 219.
[57] W. Fang-Hui, Z. Guang-Chao, W. Xian-Wen, Electrocatalytic oxidation of nitric oxide at multi-walled carbon nanotubes modified electrode, Electrochemistry Communications 4 (2002) 690.
[58] F. Wang, X. Chen, Z. Chen, Eletrodeposited nickel oxide on a film of carbon nanotubes for monitoring nitric oxide release from rat kidney and drug samples, Microchimica Acta 173 (2011) 65.
[59] P. Zhang, G.C. Zhao, X.W. Wei, Electrocatalytic oxidation of nitric oxide on an electrode modified with fullerene films, Mikrochimica Acta 149 (2005) 223.
[60] Y. Wang, Q. Li, S.S. Hu, A multiwall carbon nanotubes film-modified carbon fiber ultramicroelectrode for the determination of nitric oxide radical in liver mitochondria, Bioelectrochem 65 (2005) 135.
[61] A.R. Butler, D.L. Williams, The physiological role of nitric oxide, Chemical Society Reviews 22 (1993) 233.
[62] M. Kelm, M. Feelisch, R. Spahr, H.M. Piper, E. Noack, J. Schrader, Quantitative and kinetic characterization of nitric oxide and EDRF released from cultured endothelial cells, Biochemistry and Biophysics Research Communication 154 (1988) 236.